DMD Fast Forward. Published on July 2, 2010 as DOI: 10.1124/dmd.110.032763
DMD Fast Forward. Published on July 2, 2010 as doi:10.1124/dmd.110.032763
This article has not been copyedited and formatted. The final version may differ from this version.

Functional Expression of Carnitine/Organic Cation Transporter OCTN1/SLC22A4 in mouse small intestine and liver

Tomoko Sugiura, Sayaka Kato, Takuya Shimizu, Tomohiko Wakayama, Noritaka Nakamichi, Yoshiyuki Kubo, Daisuke Iwata, Kazuhiro Suzuki, Tomoyoshi Soga, Masahide Asano, Shoichi Iseki, Ikumi Tamai, Akira Tsuji and Yukio Kato

Faculty of Pharmacy, Institute of Medical, Pharmaceutical and Health Sciences (T.S., S.K., T.S., D.I., K.S., Y.Ku., N.N., I.T., A.T., Y.Ka.), Department of Histology and Embryology, Graduate School of Medical Science (T.W., S.I.), Division of Transgenic Animal Science, Advanced Science Research Center (M.A.), Kanazawa University, Kanazawa 920-1192, and Institute for Advanced Biosciences, Keio University, Yamagata 997-0035 (T.S.), Japan

Downloaded from dmd.aspetjournals.org at ASPET Journals on April 19, 2024

Copyright 2010 by the American Society for Pharmacology and Experimental Therapeutics.

DMD Fast Forward. Published on July 2, 2010 as DOI: 10.1124/dmd.110.032763
This article has not been copyedited and formatted. The final version may differ from this version.

Running title: OCTN1/SLC22A4 functions in small intestine and liver

Corresponding author:

Prof. Yukio Kato, Ph.D

Faculty of Pharmacy, Institute of Medical, Pharmaceutical and Health Sciences,

Kanazawa University

Kakuma-machi, Kanazawa 920-1192, Japan

Tel/Fax:(81)-76-234-4465 / Email: ykato@p.kanazawa-u.ac.jp

Document statistics:

number of text pages: 40

number of tables: 1

number of figures: 9

number of references: 40

number of words:

Abstract: 243

Introduction: 744

Discussion: 1207

Abbreviations: HEK, human embryonic kidney; OCTN1, carnitine/organic cation transporter 1; PBS, phosphatebuffered saline; SLC, solute carrier;

Downloaded from dmd.aspetjournals.org at ASPET Journals on April 19, 2024

DMD Fast Forward. Published on July 2, 2010 as DOI: 10.1124/dmd.110.032763
This article has not been copyedited and formatted. The final version may differ from this version.

ABSTRACT

Carnitine/organic cation transporter OCTN1/SLC22A4 accepts various therapeutic agents as substrates *in vitro* and is expressed ubiquitously, although its function in most organs has not yet been examined. The purpose of the present study was to evaluate functional expression of OCTN1 in small intestine and liver, using *octn1* gene knockout (*octn1*$^{-/-}$) mice. After oral administration of [^{3}H]ergothioneine ([^{3}H]ERGO), a typical substrate of OCTN1, the amount of [^{3}H]ERGO remaining in the small intestinal lumen was much higher in *octn1*$^{-/-}$ mice, compared with wild-type mice. In addition, uptake of [^{3}H]ERGO by HEK293 cells heterologously expressing OCTN1 gene product, and uptake of [^{3}H]ERGO at the apical surface of intestinal everted sacs from wild-type mice were inhibited by OCTN1 substrates, tetraethylammonium and verapamil. Immunohistochemical analysis revealed that OCTN1 is localized on the apical surface of small intestine in mice and humans. These results suggest that OCTN1 is responsible for small-intestinal absorption of [^{3}H]ERGO. However, the plasma concentration of [^{3}H]ERGO after oral administration was higher in *octn1*$^{-/-}$ mice than in wild-type mice, despite the lower absorption in *octn1*$^{-/-}$ mice. This was probably because of efficient hepatic uptake of [^{3}H]ERGO, as revealed by integration plot analysis; the uptake clearance was close to the hepatic plasma flow rate. The uptake of [^{3}H]ERGO by isolated hepatocytes was minimal, whereas [^{3}H]ERGO uptake was observed in isolated non-parenchymal cells. This is consistent with immunostaining of OCTN1 in liver sinusoids. Thus, our results indicate that OCTN1 is functionally expressed in non-parenchymal liver cells.

Downloaded from dmd.aspetjournals.org at ASPET Journals on April 19, 2024

DMD Fast Forward. Published on July 2, 2010 as DOI: 10.1124/dmd.110.032763
This article has not been copyedited and formatted. The final version may differ from this version.

INTRODUCTION

Various types of transporters have been proposed to play important roles in the absorption of nutrients and xenobiotics in small intestine. For example, hydrophilic nutrients such as saccharides, oligopeptides and hydrophilic vitamins can only minimally penetrate through the plasma membrane by passive diffusion, and specific solute carriers (SLC) are involved in their transport into epithelial cells across the apical membrane. On the other hand, hydrophobic compounds, such as many therapeutic agents and other xenobiotics, are thought to be absorbed by passive diffusion, but some of them are actively pumped out by ATP binding cassettes (ABC) transporters, thereby hindering their oral absorption. SLC transporters localized on the apical membrane of small intestine often have relatively wide substrate specificity. Consequently it has been proposed that these SLC transporters play an important role in the import of not only nutrients, but also therapeutic agents into epithelial cells. Such SLC transporters may include oligopeptide transporter (PEPT1/SLC15A), organic anion transporting polypeptide 2B1 and 1A2 in humans (Glaeser *et al.*, 2007; Groneberg *et al.*, 2001; Kobayashi *et al.*, 2003).

The presence of such influx transporters has an impact on drug development, since it may be possible to utilize them to improve the oral absorption of therapeutic agents. For example, valaciclovir, the L-valyl ester of acyclovir, was developed as a prodrug of acyclovir

Downloaded from dmd.aspetjournals.org at ASPET Journals on April 19, 2024

DMD Fast Forward. Published on July 2, 2010 as DOI: 10.1124/dmd.110.032763
This article has not been copyedited and formatted. The final version may differ from this version.

that is recognized as a substrate by PEPT1 (Balimane *et al.*, 1998). This is considered to be the reason for the greater bioavailability of valaciclovir than acyclovir (Soul-Lowton *et al*., 1995). The recognition of various types of therapeutic agents by PEPT1 has led to utilization of this transporter in rational drug design (Brandsch, 2009; Li *et al*., 2008). However, it is also important to consider influx transporter-mediated drug interactions (Banfield *et al*., 2002; Lilja *et al*., 2005a; 2005b). Lilja *et al*. (2005a; 2005b) have reported decreased plasma concentration of several ß-blockers following ingestion of citrus juice. Subsequent studies in experimental animals confirmed the presence of small intestinal influx transporters for ß-blockers (Kato *et al*., 2009; Shirasaka *et al*., 2009). However, due to the presence of other mechanism(s) also affecting oral drug absorption, the contribution of influx transporters to the overall absorption of therapeutic agents remains to be fully clarified. In addition, possible involvement of influx transporters has been demonstrated only for relatively few therapeutic agents so far, and the mechanism of membrane permeation for most orally administered drugs has not yet been clarified.

Carnitine/organic cation transporter OCTN1 (SLC22A4) was first identified in human fetal liver (Tamai *et al.*, 1997). It is ubiquitously distributed, being particularly highly expressed in the kidney, and is localized on the apical membrane of renal proximal tubular

Downloaded from dmd.aspetjournals.org at ASPET Journals on April 19, 2024

DMD Fast Forward. Published on July 2, 2010 as DOI: 10.1124/dmd.110.032763
This article has not been copyedited and formatted. The final version may differ from this version.

epithelial cells (Tamai *et al.*, 2000; Tamai *et al.*, 2003). OCTN1 transports several cationic compounds, including tetraethylammonium (TEA), pyrilamine, quinidine, verapamil, donepezil, betonicine, ergothionein (ERGO) and stachydrine (Yabuuchi *et al*., 1999; Grundemann *et al*., 2005). Gründemann *et al.* reported that ERGO was most efficiently transported by OCTN1 heterologously transfected in a mammalian cell line *in vitro* (Gründemann *et al.*, 2005). On the other hand, we have recently developed *octn1* gene knockout (*octn1*$^{-/-}$) mice and identified ERGO as a substrate of OCTN1 *in vivo* by metabolome analysis: ERGO, presumably derived from the diet, is present at μM to mM level in blood and all organs of wild-type mice, whereas its concentration was below the detection limit in *octn1*$^{-/-}$ mice, apparently because of the abrogation of OCTN1-mediated renal tubular reabsorption (Kato *et al.*, 2010). Accordingly, isotope-labeled ERGO may be a useful probe compound to analyze functional expression of OCTN1 in the body, since ERGO is not biosynthesized or metabolized in mammals (Mayumi *et al.*, 1978). However, limited information is available on the pharmacokinetics of ERGO. Further, the role of OCTN1 in most organs, except kidney, is not yet known (Urban *et al.*, 2008).

The long-term analysis (~14 days) for the plasma concentration profile of [^{3}H]ERGO in both wild-type and *octn1*$^{-/-}$ mice has already been reported (Kato *et al*., 2010),

Downloaded from dmd.aspetjournals.org at ASPET Journals on April 19, 2024

DMD Fast Forward. Published on July 2, 2010 as DOI: 10.1124/dmd.110.032763
This article has not been copyedited and formatted. The final version may differ from this version.

but the detailed mechanism underlying the difference in the plasma profile between the two strains has not yet been clarified. In the present study, we performed pharmacokinetic analysis of [^{3}H]ERGO in both wild-type and *octn1*$^{-/-}$ mice, with the aim of clarifying the role of OCTN1 in small-intestinal absorption. Since ERGO was found to be subject to predominant first-pass extraction after oral absorption, we also examined its hepatic disposition. The present study has provided the first evidence for functional expression of OCTN1 in both small intestine and liver.

Downloaded from dmd.aspetjournals.org at ASPET Journals on April 19, 2024

DMD Fast Forward. Published on July 2, 2010 as DOI: 10.1124/dmd.110.032763
This article has not been copyedited and formatted. The final version may differ from this version.

MATERIALS AND METHODS

Reagents and Animals

[^{3}H]ERGO (293 Ci/mol) and [^{14}C]inulin (2.8 μCi/mg) were obtained from Moravek Biochemicals Inc. (Brea, CA) and American Radiolabeled Chemicals Inc. (St. Louis, MO), respectivery. Sulfobromophthalein (BSP) was purchased from Sigma Aldrich Co. (St. Louis, MO). All other reagents were commercial products of reagent grade. The *octn1*$^{-/-}$ mice were generated according to the previous report (Kato *et al.*, 2010). Animals were maintained, and experiments were performed according to the Guideline for the Care and Use of Laboratory Animals in Kanazawa University.

Pharmacokinetic Studies in Mice

Male mice (6-8 weeks old) were fasted overnight with access to water, and anesthetized by intraperitoneal injection of pentobarbital. [^{3}H]ERGO at 100 or 330 μg/kg with [^{14}C]inulin (5 mg/kg) was intravenously or orally administered, respectively. Blood samples were collected at designated time intervals from the right jugular vein of each mouse and centrifuged to obtain plasma. At 4 hr after the oral administration, the mice were decapitated, and intestinal tissue was excised and divided into three parts. The radioactivity remaining

Downloaded from dmd.aspetjournals.org at ASPET Journals on April 19, 2024

DMD Fast Forward. Published on July 2, 2010 as DOI: 10.1124/dmd.110.032763
This article has not been copyedited and formatted. The final version may differ from this version.

inside the lumen was recovered by manually washing the luminal side of each segment with 5 mL of ice-cold saline using a syringe and summing up the radioactivity recovered from the three segments. At 4 hr after the intravenous injection, the mice were decapitated, and tissues were excised immediately, rinsed with about 50 mL of ice-cold saline, blotted dry, weighed and solubilized with Solene-350® (Packard Inc., Meriden, CT) at 50°C for 3 hr. The solution was treated with hydrogen peroxide and neutralized with 5 M HCl. The associated radioactivity was measured with a liquid scintillation counter, LSC-5100 (Aloka, Tokyo, Japan), with Clearsol I (Nacalai Tesque, Inc., Kyoto, Japan) as the scintillation fluid.

Integration Plot Analysis

Mice were anesthetized with pentobarbital, and [^{3}H]ERGO (100 μg/kg) was injected via the left jugular vein. Blood was withdrawn from the right jugular vein at designated times, and plasma was separated by centrifugation. After 1, 2, 3 or 5 minutes, the mice were sacrificed, and liver was obtained and solubilized. The solubilized liver and plasma were each mixed with scintillation liquid, and the associated radioactivity was measured with a liquid scintillation counter as described above. Efflux from the liver soon after intravenous administration was assumed to be negligible, and the tissue uptake clearance (CL_{uptake}) was

Downloaded from dmd.aspetjournals.org at ASPET Journals on April 19, 2024

DMD Fast Forward. Published on July 2, 2010 as DOI: 10.1124/dmd.110.032763
This article has not been copyedited and formatted. The final version may differ from this version.

calculated with the following equation:

$$\frac{X_T(t)}{Cp(t)} = CL_{uptake} \cdot \frac{AUC}{Cp(t)} + V0$$

where $X_T(t)$ and Cp(t) are the tissue amount and the plasma concentration at time t, respectively. AUC is the area under the plasma concentration-time curve. V_0 is the volume of distribution, within which a rapid equilibrium with the plasma compartment is assumed. When $\frac{X_T(t)}{Cp(t)}$ is plotted against $\frac{AUC}{Cp(t)}$, the slope represents the value of CL_{uptake}.

Uptake of [^{3}H]ERGO by Everted Intestinal Sac

The experimental procedure was as described previously (Nakashima *et al*., 1984). The freshly isolated small intestine was equally divided into upper, middle and lower segments. Each intestinal segment was everted with polyethylene tubing, and the everted sacs were washed with the buffer solution. After 5 min preincubation, the sacs were incubated with [^{3}H]ERGO (40 nM) and an extracellular marker, [^{14}C]inulin for 10 min. Then, they were washed with ice-cold buffer solution, blotted dry, weighed, and solubilized. The associated radioactivity was measured as described above. The buffer solution was composed of (mM): 123 NaCl, 5.1 KCl, 1.4 $CaCl_2$, 1.3 $MgSO_4$, 21 $NaHCO_3$, 1.3 KH_2PO_4, and 5 D-glucose, adjusted at pH 6.0, maintained at 37 °C and gassed with O_2 before and during the experiment.

Downloaded from dmd.aspetjournals.org at ASPET Journals on April 19, 2024

DMD Fast Forward. Published on July 2, 2010 as DOI: 10.1124/dmd.110.032763
This article has not been copyedited and formatted. The final version may differ from this version.

Transport Studies in HEK293/OCTN1 Cells

Plasmid DNA encoding mouse OCTN1 was transiently transfected into HEK293 cells according to the calcium phosphate precipitation method (Tamai *et al*., 2000). At 48 hr after transfection, the HEK293/OCTN1 cells were harvested and suspended in the transport buffer (125 mM NaCl, 4.8 mM KCl, 5.6 mM D-glucose, 1.2 mM $CaCl_2$, 1.2 mM KH_2PO_4, 1.2 mM $MgSO_4$, and 25 mM HEPES, pH 7.4). The uptake experiment was then performed according to the silicone oil layer method (Tamai *et al*., 2000).

Isolation and Transport Experiments in Nonparenchymal Liver Cells

The separation of liver parenchymal and nonparenchymal cells was performed by the collagenase perfusion method (Berry and Friend, 1969; Horiuchi *et al*., 1985) with some modifications. Briefly, mice were anesthetized with pentobarbital, and their body temperature was maintained at 37˚C during the experiment. The liver was perfused first with Ca^{2+}, Mg^{2+}-free buffer from the inferior vena cava for 3 min, followed by perfusion buffer containing 5 mM $CaCl_2$, 0.03% collagenase and 0.005% trypsin inhibitor for 10 min. As soon as the perfusion was started, the portal vein was cut, and the perfusion rate was maintained at

Downloaded from dmd.aspetjournals.org at ASPET Journals on April 19, 2024

DMD Fast Forward. Published on July 2, 2010 as DOI: 10.1124/dmd.110.032763
This article has not been copyedited and formatted. The final version may differ from this version.

4 mL/min. The dispersed liver cells were separated into parenchymal and nonparenchymal cells (PC and NPC, respectively) by differential centrifugation. The isolated cells were resuspended in ice-cold transport buffer. After incubation with [^{3}H]ERGO (40 nM), the mixture was 10-fold diluted with ice-cold transport buffer, then centrifuged for 1 min, and the supernatant was removed. The cells were washed three times with ice-cold buffer, followed by solubilization with NaOH. After solubilization, the cell lysate was neutralized with HCl. The associated radioactivity was measured as described above. Cellular protein content was determined with a protein assay kit (Bio-Rad, Hercules, CA). The quantification of BSP was performed by HPLC (LC-10A series; Shimadzu, Kyoto, Japan). The reversed-phase column (COSMOSIL 5C_{18}-AR-II, 4.6 x 150 mm; Nacalai Tesque, Kyoto, Japan) was maintained at 40˚C in a column oven. The mobile phase was a mixture of 20 mM potassium phosphate buffer (pH 6.0) and acetonitrile (70:30). The UV detector was set at 230 nm. The flow rate was 1.0 mL/min.

Immunohistochemical Studies and Western blot analysis

Mice were anesthetized and transcardially perfused with 4% paraformaldehyde (PFA). The liver and small intestine were removed and sequentially immersed in 4% PFA, 10,

Downloaded from dmd.aspetjournals.org at ASPET Journals on April 19, 2024

DMD Fast Forward. Published on July 2, 2010 as DOI: 10.1124/dmd.110.032763
This article has not been copyedited and formatted. The final version may differ from this version.

20 and 30% sucrose/PBS. The tissue was then frozen and sectioned with a cryostat, and the sections (10 μm) were mounted on glass slides. Slides of 4 μm sections of formalin-fixed, paraffin-embedded normal human small intestinal tissue were purchased from COSMO BIO Co., Ltd. (Tokyo, Japan). The slides were then incubated with a mixture of first antibodies at 4˚C overnight and further incubated with secondary antibodies (Alexa Fluor 488 goat anti-mouse, Alexa Fluor 488 goat anti-rat and Alexa Fluor 594 anti-rabbit IgG conjugates) (Molecular Probes Inc., Eugene, OR) for 30 min at room temperature. Finally, they were mounted in VECTASHIELD mounting medium with DAPI (Vector Laboratories, Burlingame, CA) to fix the sample and to stain nuclei. The specimens were examined with a confocal laser scanning fluorescence microscope (LSM 510; Carl Zeiss, Jena, Germany). Mouse intestinal brush border membrane vesicles (BBMVs) were prepared according to the previous study (Sugiura *et al.*, 2008). Hepatic NPC, PC and HEK293/OCTN1 cells were obtained as described above. These samples were solubilized in RIPA-Y buffer containing 1% Nonidet P-40, 75 mM NaCl, 50 mM Tris-HCl, pH 7.5 and protease inhibitors. Solubilized samples were analyzed by SDS-polyacrylamide gel electrophoresis (SDS-PAGE), followed by immunoblotting with antisera against OCTN1. Western blot analysis was performed as described previously (Kato *et al*., 2005).

Downloaded from dmd.aspetjournals.org at ASPET Journals on April 19, 2024

DMD Fast Forward. Published on July 2, 2010 as DOI: 10.1124/dmd.110.032763
This article has not been copyedited and formatted. The final version may differ from this version.

Statistical Analysis

Statistical analyses were performed by means of Student's *t*-test or ANOVA with Tukey's post hoc comparison test for single and multiple comparisons, respectively. Differences were considered statistically significant at $p < 0.05$.

Downloaded from dmd.aspetjournals.org at ASPET Journals on April 19, 2024

DMD Fast Forward. Published on July 2, 2010 as DOI: 10.1124/dmd.110.032763
This article has not been copyedited and formatted. The final version may differ from this version.

RESULTS

Absorption and Uptake from Apical Side of [^{3}H]ERGO in Small Intestine

To investigate the role of OCTN1 in the small intestine, [^{3}H]ERGO was first orally administered to wild-type and *octn1*$^{-/-}$ mice, and radioactivity remaining inside the small intestinal lumen was measured in order to estimate gastrointestinal absorption. Less than 3% of the dose was recovered in the gastrointestinal tract of wild-type mice, whereas approximately 30% of the dose remained in *octn1*$^{-/-}$ mice (Figure 1A). On the other hand, the recovery of [^{14}C]inulin was not very different between the two strains (39.6 ± 2.3 and 52.7 ± 2.8% of the dose in wild-type and *octn1*$^{-/-}$ mice, respectively). These results suggest that gastrointestinal absorption of [^{3}H]ERGO was reduced in *octn1*$^{-/-}$ mice.

To further compare the small-intestinal membrane permeability of [^{3}H]ERGO in wild-type and *octn1*$^{-/-}$ mice, uptake of [^{3}H]ERGO from the apical side of the small intestine was measured by means of the everted sac method. [^{3}H]ERGO uptake was observed in the upper, middle and lower parts of the small intestine of wild-type mice, whereas that in *octn1*$^{-/-}$ mice was much lower (Figure 2A). The uptake of [^{3}H]ERGO by everted sacs of wild-type mice was reduced in the presence of unlabeled ERGO in a concentration-dependent manner (Figure 2B). Further, the [^{3}H]ERGO uptake in wild-type mice was reduced in the presence of

Downloaded from dmd.aspetjournals.org at ASPET Journals on April 19, 2024

DMD Fast Forward. Published on July 2, 2010 as DOI: 10.1124/dmd.110.032763
This article has not been copyedited and formatted. The final version may differ from this version.

TEA or verapamil, both of which are substrates for OCTN1 (Figure 3A).

Characterization of the Uptake of [^{3}H]ERGO by OCTN1

The uptake of [^{3}H]ERGO by mouse OCTN1 was characterized using HEK293/OCTN1 cells. The OCTN1-mediated uptake of [^{3}H]ERGO, obtained by subtracting the uptake in vector-transfected HEK293 cells from that in HEK293/OCTN1 cells, was reduced in the presence of TEA and verapamil (Figure 3B). Such an inhibition profile is similar to that in the case of [^{3}H]ERGO uptake in mouse small intestine (Figure 3A, 3B).

Expression and Localization of OCTN1 in Small Intestine

Localization of OCTN1 in the small intestine was next investigated by immunohistochemistry (Figure 4A-J). OCTN1 was detected on apical region of epithelial cells in wild-type mice (Figure 4A, 4E), but not in *octn1*$^{-/-}$ mice (Figure 4C). OCTN1 was also detected in the intestinal crypts (Figure 4A). Anti Na^+/K^+-ATPase antibody was used as a basolateral membrane marker (Figure 4F), and the OCTN1 signal was distinct from that of Na^+/K^+-ATPase, as revealed by double staining of the two membrane proteins (Figure 4G). Additionally, to confirm apical localization of OCTN1, colocalization with PDZK1, an apical

Downloaded from dmd.aspetjournals.org at ASPET Journals on April 19, 2024

DMD Fast Forward. Published on July 2, 2010 as DOI: 10.1124/dmd.110.032763
This article has not been copyedited and formatted. The final version may differ from this version.

membrane scaffold protein was further examined. Double labeled immunohistochemistry with antisera against OCTN1 and PDZK1 yielded merged signals, indicating apical localization of OCTN1 (Figure 4H, I, J). This is further supported by the detection of OCTN1 gene product in the small intestinal BBMVs in Western blot analysis (Figure 4K). Expression of OCTN1 was also examined in human small intestine, and was again detected on the apical membrane (Figure 5).

First-pass Uptake of [^{3}H]ERGO in Liver

Based on the data shown in Figures 1A, 2 and 3, the plasma concentration of [^{3}H]ERGO in *octn1*$^{-/-}$ mice after oral administration was expected to be lower than that in wild-type mice. In our previous experiments, however, we found that the plasma concentration of [^{3}H]ERGO after oral administration was transiently higher in *octn1*$^{-/-}$ mice compared with that in wild-type mice (Kato *et al*., 2010). Since the oral absorption profile was not further examined during the short time period covered in the previous analysis, we next examined the plasma concentration profile of [^{3}H]ERGO until 4 hr after oral administration. Plasma concentration of [^{3}H]ERGO in *octn1*$^{-/-}$ mice was higher than that in wild-type mice immediately after oral administration (Figure 1B), confirming our previous

Downloaded from dmd.aspetjournals.org at ASPET Journals on April 19, 2024

DMD Fast Forward. Published on July 2, 2010 as DOI: 10.1124/dmd.110.032763
This article has not been copyedited and formatted. The final version may differ from this version.

observation (Kato *et al.*, 2010). A possible explanation of this would be efficient hepatic first-pass extraction of [^{3}H]ERGO in wild-type, but not in *octn1*$^{-/-}$ mice. To examine this hypothesis, [^{3}H]ERGO was intravenously injected, and its distribution to the liver was compared in wild-type and *octn1*$^{-/-}$ mice. After the intravenous injection, plasma [^{3}H]ERGO initially fell rapidly in wild-type mice and then declined with a longer half-life, while that in *octn1*$^{-/-}$ mice showed a gradual and continuous decrease (Figure 6A). The more rapid elimination phase in *octn1*$^{-/-}$ mice (Figure 6A) was compatible with much higher urinary excretion in *octn1*$^{-/-}$ mice (Figure 6B). The hepatic uptake process of [^{3}H]ERGO was then investigated by integration plot analysis (Figure 7). The integration plot for hepatic uptake of [^{3}H]ERGO showed an almost linear increase in wild-type mice, but that in *octn1*$^{-/-}$ mice showed only a minimal increase (Figure 7). CL_{uptake} of [^{3}H]ERGO in wild-type mice was estimated to be 1.07 mL/min/g tissue, whereas that in *octn1*$^{-/-}$ mice was 0.0145 mL/min/g tissue. Efficient hepatic uptake was also supported by the fact that the highest value of tissue-to-plasma concentration ratio (Kp) of [^{3}H]ERGO was measured at 4 hr after intravenous administration (Table 1). In addition to the liver, the Kp values of [^{3}H]ERGO in kidney, spleen, lung, heart, small intestine, large intestine, testis, pancreas, thymus and bone marrow of *octn1*$^{-/-}$ mice were significantly lower than those in wild-type mice (Table 1).

Downloaded from dmd.aspetjournals.org at ASPET Journals on April 19, 2024

DMD Fast Forward. Published on July 2, 2010 as DOI: 10.1124/dmd.110.032763
This article has not been copyedited and formatted. The final version may differ from this version.

Uptake of [^{3}H]ERGO, Expression and Localization of OCTN1 in NPC

To evaluate which fraction of the liver cells contributes to the hepatic uptake of [^{3}H]ERGO, we next performed an uptake study using freshly isolated hepatic PC and NPC. In PC of wild-type mice, uptake of [^{3}H]ERGO was almost negligible, being similar to that of [^{14}C]inulin, whereas strong uptake of BSP was observed (Figure 8A). On the other hand, [^{3}H]ERGO was taken up into NPC isolated from wild-type mice in a time-dependent manner, but uptake into NPC of *octn1*$^{-/-}$ mice was much lower and showed minimal time dependence (Figure 8B). The localization of OCTN1 in the liver was then investigated by immunohistochemical analysis (Figure 9). A fluorescence signal corresponding to OCTN1 was observed in sinusoidal vessels, but not on plasma membranes of hepatocytes (Figure 9A, D). Anti-CD31 antibody was used as an endothelial cell marker (Figure 9B, E), and its signal at least partially overlapped with that of OCTN1 in wild-type mice (Figure 9C, F, G). Furthermore, Western blot analysis detected the band of OCTN1 gene product in the hepatic NPC, but not in that of PC (Figure 4K), supporting the higher transport activity of [^{3}H]ERGO in NPC compared with PC of wild-type mice.

Downloaded from dmd.aspetjournals.org at ASPET Journals on April 19, 2024

DMD Fast Forward. Published on July 2, 2010 as DOI: 10.1124/dmd.110.032763
This article has not been copyedited and formatted. The final version may differ from this version.

DISCUSSION

ERGO is a natural thiol compound present in mushrooms and mammalian tissues (Ey *et al.*, 2007). Biosynthesis of ERGO occurs only in certain microorganisms, and so ERGO is presumably absorbed from daily foods in mammals. Since the membrane permeability of ERGO is expected to be limited due to its hydrophilicity, it is reasonable to speculate that a transporter is involved in its gastrointestinal absorption. However, there has been no report on the oral absorption mechanism of this compound. Here, we found that when [^{3}H]ERGO was orally administered to wild-type and *octn1*$^{-/-}$ mice, a greater amount of [^{3}H]ERGO remained in the gastrointestinal tract of *octn1*$^{-/-}$ mice, and the amount remaining in wild-type mice was quite small (Figure 1A). These observations indicate the involvement of OCTN1 in absorption of ERGO from the luminal side of the small intestine. This conclusion was further supported by uptake studies of [^{3}H]ERGO using the everted sac method (Figures 2 and 3): [^{3}H]ERGO was efficiently taken up by intestinal tissue in wild-type mice, but the uptake in *octn1*$^{-/-}$ mice was negligible (Figure 2A). The uptake of [^{3}H]ERGO by everted sacs of wild-type mice was reduced in the presence of unlabeled ERGO (Figure 2B), and this concentration dependence was consistent with the reported Km value of mouse OCTN1 for ERGO (~5 μM, Kato *et al.*, 2010). TEA and verapamil, both of which are substrates of

Downloaded from dmd.aspetjournals.org at ASPET Journals on April 19, 2024

DMD Fast Forward. Published on July 2, 2010 as DOI: 10.1124/dmd.110.032763
This article has not been copyedited and formatted. The final version may differ from this version.

OCTN1, also inhibited the uptake of [^{3}H]ERGO by everted sacs, and the inhibition pattern is similar to that found in HEK293/OCTN1 cells (Figure 3). Finally, immunostaining for OCTN1 was detected on the small-intestinal apical membrane of wild-type mice (Figure 4A-J) and humans (Figure 5). This apical localization of OCTN1 was further confirmed by Western blot analysis of intestinal BBMVs (Figure 4K). All these findings indicate that OCTN1 is functionally expressed on the apical membrane of small intestinal epithelial cells *in vivo*.

The OCTN1-mediated ERGO uptake at small-intestinal apical membrane was inhibited by a therapeutic agent, verapamil (Figure 3). In view of the wide substrate specificity of OCTN1 (Yabuuchi *et al*., 1999; Grundemann *et al*., 2005), the apical localization of this transporter both in humans and mice may require further consideration of the contribution of OCTN1 to oral absorption of other therapeutic agents; indeed, this transporter might be a novel target for rational design of orally administrable drugs. OCTN1 can act as an exchanger for H^+ and organic cations in *OCTN1* gene-transfected HEK293 cells (Tamai *et al*., 2004). On the other hand, some cationic compounds, such as cimetidine and guanidine, were reported to be transported via H^+/cation exchange mechanisms across the brush border membranes in small intestine, but the transport properties seem not to be fully

Downloaded from dmd.aspetjournals.org at ASPET Journals on April 19, 2024

DMD Fast Forward. Published on July 2, 2010 as DOI: 10.1124/dmd.110.032763
This article has not been copyedited and formatted. The final version may differ from this version.

consistent with those of OCTN1 (Piyapolrungroj *et al*., 1999).

The plasma concentration profile of [^{3}H]ERGO in *octn1*$^{-/-}$ mice until 4 hr after oral administration was unexpectedly higher than that in wild-type mice (Figure 1B), in spite of the lower intestinal absorption of [^{3}H]ERGO in *octn1*$^{-/-}$ mice (Figure 1A). To elucidate this apparent inconsistency, we examined hepatic extraction of [^{3}H]ERGO. Integration plot analysis (Figure 7) revealed continuous uptake of [^{3}H]ERGO in the liver of wild-type mice, and the CL_{uptake} was estimated to be ~ 1 mL/min /g tissue, which is close to the hepatic plasma flow rate (Davies and Morris, 1993). Thus, the hepatic uptake of ERGO in wild-type mice seems to be blood flow-limited. On the other hand, the integration plot for *octn1*$^{-/-}$ mice revealed almost negligible uptake (Figure 7). Therefore, lower hepatic extraction in *octn1*$^{-/-}$ mice (Figure 7) may over-compensate for the lower oral absorption (Figure 1A), leading to a higher concentration of [^{3}H]ERGO in the systemic circulation of *octn1*$^{-/-}$ mice (Figure 1B). Furthermore, hepatic NPC, but not PC, seem to play a crucial role in the efficient uptake of [^{3}H]ERGO in the liver (Figure 8). This was supported by the overlap of immunostainings for OCTN1 and an endothelial cell marker CD31, while hepatocytes were not stained for OCTN1 (Figure 9). The detection of OCTN1 by Western blot analysis in NPC, but not in PC of wild-type mice (Figure 4K) was also consistent with the transport activity of [^{3}H]ERGO by

Downloaded from dmd.aspetjournals.org at ASPET Journals on April 19, 2024

DMD Fast Forward. Published on July 2, 2010 as DOI: 10.1124/dmd.110.032763
This article has not been copyedited and formatted. The final version may differ from this version.

NPC (Figure 8). It seems be noteworthy that NPC account for only 1/3 of total liver cells, but are responsible for a more than 200 times higher concentration of [^{3}H]ERGO in the liver (Kp ~ 238) compared with the systemic circulation. This means that ERGO is highly concentrated inside NPC. Although the physiological role of ERGO in NPC should be clarified by further analyses, ERGO is a very stable antioxidant and is capable of scavenging reactive oxygen species (Melville, 1958; Hartman, 1990). Liver sinusoidal endothelial cells are the primary sites of phagocyte attachment and play an important role in defense against phagocyte-derived reactive oxygen species (Spolarics, 1998). Dysfunction of the liver sinusoidal cells has been observed during arsenic-induced oxidative stress, leading to vascular disease atherosclerosis (States *et al*., 2009). Bedirli *et al.* (2004) have demonstrated that exogenous administration of ERGO improves survival in animals with liver injury induced by ischemia and reperfusion. Thus, ERGO may function as one of the defense mechanisms acting under such pathological conditions. The present findings, however, do not rule out the possible existence of OCTN1 in other NPC than endothelial cells. More detailed studies are required to understand the role of OCTN1.

A substantial amount of [^{3}H]ERGO was orally absorbed even in *octn1*$^{-/-}$ mice (Figure 1B), indicating a contribution of other membrane permeation mechanism(s) at the

Downloaded from dmd.aspetjournals.org at ASPET Journals on April 19, 2024

DMD Fast Forward. Published on July 2, 2010 as DOI: 10.1124/dmd.110.032763
This article has not been copyedited and formatted. The final version may differ from this version.

apical membrane of the small intestine. Considering the hydrophilicity of ERGO, passive diffusion through lipid bilayers is unlikely to be significant. Although OCTN2 is also expressed on apical membrane of small intestinal epithelial cells (Kato *et al.*, 2006), [^{3}H]ERGO was not transported by HEK293 cells transfected with mouse OCTN2 (Kato *et al.*, 2010). OCTN3 is another member of the OCTN family, but is expressed on the basolateral membrane in the small intestine (Durán *et al.*, 2005). Accordingly, some other transporter(s) localized on the apical membrane of small intestine is likely to be involved in intestinal absorption of ERGO. The presence of other influx transporters for ERGO was also supported by the present finding in everted sacs that a part of the uptake of [^{3}H]ERGO is not inhibited even in the presence of 100 μM unlabeled ERGO (Figure 2B). Thus, the present findings indicate the presence of multiple influx transporters for ERGO on small-intestinal apical membrane.

After intravenous administration to wild-type mice, [^{3}H]ERGO rapidly disappeared from the circulation in the initial phase (Figure 6A). Such rapid elimination can probably be explained by large tissue distribution of [^{3}H]ERGO (Table 1). For example, hepatic distribution (Kp, ~ 240 mL/g tissue, Table 1) can account for the distribution volume of ~10 liter/kg in wild-type mice, but was negligible in *octn1*$^{-/-}$ mice (Figure 7, Table 1). This may

Downloaded from dmd.aspetjournals.org at ASPET Journals on April 19, 2024

DMD Fast Forward. Published on July 2, 2010 as DOI: 10.1124/dmd.110.032763
This article has not been copyedited and formatted. The final version may differ from this version.

lead to relatively rapid elimination in the terminal phase in *octn1*$^{-/-}$ mice (Figure 6A). Such an OCTN1-mediated pharmacokinetic profile of ERGO would be quite similar to the OCTN2-mediated disposition of carnitine, which was clarified by the use of wild-type and *octn2* mutant mice (Yokogawa *et al.*, 1999): OCTN2 contributes to intestinal absorption, tissue distribution and renal tubular reabsorption of carnitine (Yokogawa *et al.*, 1999a; Kato *et al.*, 2006), as seen in the case of ERGO and OCTN1.

Downloaded from dmd.aspetjournals.org at ASPET Journals on April 19, 2024

DMD Fast Forward. Published on July 2, 2010 as DOI: 10.1124/dmd.110.032763
This article has not been copyedited and formatted. The final version may differ from this version.

ACKNOWLEDGEMENT

We thank Ms Lica Ishida for technical assistance. We also thank Mr Kazuki Matsubara and Takayuki Taguchi for isolation of liver cells and uptake experiments, respectively.

Downloaded from dmd.aspetjournals.org at ASPET Journals on April 19, 2024

DMD Fast Forward. Published on July 2, 2010 as DOI: 10.1124/dmd.110.032763
This article has not been copyedited and formatted. The final version may differ from this version.

REFERENCES

Balimane PV, Tamai I, Guo A, Nakanishi T, Kitada H, Leibach FH, Tsuji A and Sinko PJ (1998) Direct evidence for peptide transporter (PepT1)-mediated uptake of a nonpeptide prodrug, valacyclovir. *Biochem Biophys Res Commun* **250**: 246-251

Berry MN and Friend DS (1969) High-yield preparation of isolated rat liver parenchymal cells: a biochemical and fine structural study. *J Cell Biol* **43**: 506-520.

Bedirli A, Sakrak O, Muhtaroglu S, Soyuer I, Guler I, Riza Erdogan A and Sozuer EM (2004) Ergothioneine pretreatment protects the liver from ischemia-reperfusion injury caused by increasing hepatic heat shock protein 70. *J Surg Res* **122**: 96 –102.

Blomhoff R, Blomhoff HK, Tolleshaug H, Christensen TB and Berg T (1985) Uptake and degradation of bovine testes beta-galactosidase by parenchymal and nonparenchymal rat liver cells. *Int J Biochem* **17**: 1321-1328.

Brandsch M (2009) Transport of drugs by proton-coupled peptide transporters: pearls and pitfalls. *Expert Opin Drug Metab Toxicol* **5**: 887-905.

Banfield C, Gupta S, Marino M, Lim J and Affrime M (2002) Grapefruit juice reduces the oral bioavailability of fexofenadine but not desloratadine. *Clin Pharmacokinet* **41**: 311-318.

Downloaded from dmd.aspetjournals.org at ASPET Journals on April 19, 2024

DMD Fast Forward. Published on July 2, 2010 as DOI: 10.1124/dmd.110.032763
This article has not been copyedited and formatted. The final version may differ from this version.

Davies B and Morris T (1993) Physiological parameters in laboratory animals and humans. *Pharm Res* **10**: 1093-1095.

Durán JM, Peral MJ, Calonge ML and Ilundáin AA (2005) OCTN3: A Na+-independent L-carnitine transporter in enterocytes basolateral membrane. *J Cell Physiol* **202**: 929-935.

Ey J, Schömig E and Taubert D (2007) Dietary sources and antioxidant effects of ergothioneine. *J Agric Food Chem* **55**: 6466-6474.

Glaeser H, Bailey DG, Dresser GK, Gregor JC, Schwarz UI, McGrath JS, Jolicoeur E, Lee W, Leake BF, Tirona RG and Kim RB (2007) Intestinal drug transporter expression and the impact of grapefruit juice in humans. *Clin Pharmacol Ther* **81**: 362-370.

Groneberg DA, Döring F, Eynott PR, Fischer A and Daniel H (2001) Intestinal peptide transport: ex vivo uptake studies and localization of peptide carrier PEPT1. *Am J Physiol Gastrointest Liver Physiol* **281**: G697-704.

Gründemann D, Harlfinger S, Golz S, Geerts A, Lazar A, Berkels R, Jung N, Rubbert A and Schömig E (2005) Discovery of the ergothioneine transporter. *Proc Natl Acad Sci* **102** 5256-5261.

Hartman PE (1990) Ergothioneine as antioxidant. *Methods Enzymol* **186**: 310-318.

Downloaded from dmd.aspetjournals.org at ASPET Journals on April 19, 2024

DMD Fast Forward. Published on July 2, 2010 as DOI: 10.1124/dmd.110.032763
This article has not been copyedited and formatted. The final version may differ from this version.

Horiuchi S, Takata K and Morino Y (1985) Characterization of a membrane-associated receptor from rat sinusoidal liver cells that binds formaldehyde-treated serum albumin. *J Biol Chem* **260**: 475-481.

Kano T, Kato Y, Ito K, Ogihara T, Kubo Y and Tsuji A (2009) Carnitine/organic cation transporter OCTN2 (Slc22a5) is responsible for renal secretion of cephaloridine in mice. *Drug Metab Dispos* **37**: 1009-1016

Kato Y, Kubo Y, Iwata D, Kato S, Sudo T, Sugiura T, Kagaya T, Wakayama T, Hirayama A, Sugimoto M, Sugihara K, Kaneko S, Soga T, Asano M, Tomita M, Matsui T, Wada M and Tsuji1 A. (2010) Gene Knockout and Metabolome Analysis of Carnitine/Organic Cation Transporter OCTN1 (SLC22A4). *Pharm Res* **27**: 832-840

Kato Y, Miyazaki T, Kano T, Sugiura T, Kubo Y and Tsuji A (2009) Involvement of influx and efflux transport systems in gastrointestinal absorption of celiprolol. *J Pharm Sci* **98**: 2529-2539.

Kato Y, Sai Y, Yoshida K, Watanabe C, Hirata T, and Tsuji A (2005) PDZK1 directly regulates the function of organic cation/carnitine transporter OCTN2. *Mol Pharmacol* **67**: 734-743.

Kato Y, Sugiura M, Sugiura T, Wakayama T, Kubo Y, Kobayashi D, Sai Y, Tamai I, Iseki S

Downloaded from dmd.aspetjournals.org at ASPET Journals on April 19, 2024

DMD Fast Forward. Published on July 2, 2010 as DOI: 10.1124/dmd.110.032763
This article has not been copyedited and formatted. The final version may differ from this version.

and Tsuji A (2006) Organic cation/carnitine transporter OCTN2 (Slc22a5) is responsible for carnitine transport across apical membranes of small intestinal epithelial cells in mouse. *Mol Pharmacol* **70**: 829-837.

Kobayashi D, Nozawa T, Imai K, Nezu J, Tsuji A and Tamai I (2003) Involvement of human organic anion transporting polypeptide OATP-B (SLC21A9) in pH-dependent transport across intestinal apical membrane. *J Pharmacol Exp Ther* **306**: 703-708.

Li F, Maag H and Alfredson T (2008) Prodrugs of nucleoside analogues for improved oral absorption and tissue targeting. *J Pharm Sci* **97**: 1109-1134.

Lilja JJ, Raaska K and Neuvonen PJ (2005a) Effects of grapefruit juice on the pharmacokinetics of acebutolol. *Br J Clin Pharmacol* **60**: 659-663

Lilja JJ, Raaska K and Neuvonen PJ (2005b) Effects of orange juice on the pharmacokinetics of atenolol. *Eur J Clin Pharmacol* **61**: 337-340

Mayumi T, Kawano H, Sakamoto Y, Suehisa E, Kawai Y and Hama T (1978) Studies on ergothioneine V. Determination by high performance liquid chromatography and application to metabolic research. *Chem Pharm Bull* (Tokyo) **26**: 3772-3778

Melville DB (1958) L-Ergothioneine. *Vitam Horm* **17**: 155-204

Nakashima E, Tsuji A, Mizuo H and Yamana T (1984) Kinetics and mechanism of in vitro

Downloaded from dmd.aspetjournals.org at ASPET Journals on April 19, 2024

DMD Fast Forward. Published on July 2, 2010 as DOI: 10.1124/dmd.110.032763
This article has not been copyedited and formatted. The final version may differ from this version.

uptake of amino-beta-lactam antibiotics by rat small intestine and relation to the intact-peptide transport system. *Biochem Pharmacol* **33:** 3345–3352.

Nezu J, Tamai I, Oku A, Ohashi R, Yabuuchi H, Hashimoto N, Nikaido H, Sai Y, Koizumi A, Shoji Y, Takada G, Matsuishi T, Yoshino M, Kato H, Ohura T, Tsujimoto G, Hayakawa J, Shimane M and Tsuji A (1999) Primary systemic carnitine deficiency is caused by mutations in a gene encoding sodium ion-dependent carnitine transporter. *Nat Genet* **21**: 91-94.

Piyapolrungroj N, Li C, Pisoni RL and Fleisher D (1999) Cimetidine transport in brush-border membrane vesicles from rat small intestine. *J Pharmacol Exp Ther* **289**: 346-353.

Shirasaka Y, Li Y, Shibue Y, Kuraoka E, Spahn-Langguth H, Kato Y, Langguth P and Tamai I (2009) Concentration-dependent effect of naringin on intestinal absorption of beta(1)-adrenoceptor antagonist talinolol mediated by p-glycoprotein and organic anion transporting polypeptide (Oatp). *Pharm Res* **26**: 560-567.

Soul-Lawton J, Seaber E, On N, Wootton R, Rolan P and Posner J (1995) Absolute bioavailability and metabolic disposition of valaciclovir, the L-valyl ester of acyclovir, following oral administration to humans. *Antimicrob Agents Chemother* **39**: 2759-2764

Spolarics Z (1998) Endotoxemia, pentose cycle, and the oxidant/antioxidant balance in the

Downloaded from dmd.aspetjournals.org at ASPET Journals on April 19, 2024

DMD Fast Forward. Published on July 2, 2010 as DOI: 10.1124/dmd.110.032763
This article has not been copyedited and formatted. The final version may differ from this version.

hepatic sinusoid. *J Leukoc Biol* **63**: 534-541.

States JC, Srivastava S, Chen Y and Barchowsky A (2009) Arsenic and cardiovascular disease. *Toxicol Sci* **107**: 312-323.

Sugiura T, Kato Y, Wakayama T, Silver DL, Kubo Y, Iseki S, and Tsuji A (2008) PDZK1 regulates two intestinal solute carriers (Slc15a1 and Slc22a5) in mice. *Drug Metab Dispos* **36**: 1181-1188.

Tamai I, Ohashi R, Nezu JI, Sai Y, Kobayashi D, Oku A, Shimane M and Tsuji A (2000) Molecular and functional characterization of organic cation/carnitine transporter family in mice. *J Biol Chem* **275**: 40064-40072.

Tamai I, Nakanishi T, Kobayashi D, China K, Kosugi Y, Nezu J, Sai Y and Tsuji A (2003) Involvement of OCTN1 (SLC22A4) in pH-dependent transport of organic cations. *Mol Pharm* **1**: 57-66.

Tamai I, Yabuuchi H, Nezu J, Sai Y, Oku A, Shimane M and Tsuji A (1997) Cloning and characterization of a novel human pH-dependent organic cation transporter, OCTN1. *FEBS Lett* **419**: 107-111.

Urban TJ, Brown C, Castro RA, Shah N, Mercer R, Huang Y, Brett CM, Burchard EG and Giacomini KM (2008) Effects of genetic variation in the novel organic cation

Downloaded from dmd.aspetjournals.org at ASPET Journals on April 19, 2024

DMD Fast Forward. Published on July 2, 2010 as DOI: 10.1124/dmd.110.032763
This article has not been copyedited and formatted. The final version may differ from this version.

transporter, OCTN1, on the renal clearance of gabapentin. *Clin Pharmacol Ther* **83**: 416-421.

Yabuuchi H, Tamai I, Nezu J, Sakamoto K, Oku A, Shimane M, Sai Y and Tsuji A (1999) Novel Membrane Transporter OCTN1 Mediates Multispecific, Bidirectional, and pH-Dependent Transport of Organic Cations. *J Pharmacol Exp Ther* **289**: 768-773

Yokogawa K, Higashi Y, Tamai I, Nomura M, Hashimoto N, Nikaido H, Hayakawa J, Miyamoto K and Tsuji A (1999a) Decreased tissue distribution of L-carnitine in juvenile visceral steatosis mice. *J Pharmacol Exp Ther* **289**: 224-230.

Yokogawa K, Yonekawa M, Tamai I, Ohashi R, Tatsumi Y, Higashi Y, Nomura M, Hashimoto N, Nikaido H, Hayakawa J, Nezu J, Oku A, Shimane M, Miyamoto K and Tsuji A (1999b) Loss of wild-type carrier-mediated L-carnitine transport activity in hepatocytes of juvenile visceral steatosis mice. *Hepatology* **30**: 997-1001.

Downloaded from dmd.aspetjournals.org at ASPET Journals on April 19, 2024

DMD Fast Forward. Published on July 2, 2010 as DOI: 10.1124/dmd.110.032763
This article has not been copyedited and formatted. The final version may differ from this version.

FOOTNOTES

This study was supported in part by a Grant-in-Aid for Scientific Research provided by the Ministry of Education, Science and Culture of Japan and in part by the Japan Research Foundation for Clinical Pharmacology.

Downloaded from dmd.aspetjournals.org at ASPET Journals on April 19, 2024

DMD Fast Forward. Published on July 2, 2010 as DOI: 10.1124/dmd.110.032763
This article has not been copyedited and formatted. The final version may differ from this version.

LEGENDS FOR FIGURES

Figure 1

Amount remaining in intestinal lumen (A) and plasma concentration-time course (B) of [^{3}H]ERGO after oral administration.

(A) [^{3}H]ERGO was orally administered to wild-type (closed symbols) and *octn1*$^{-/-}$ (open symbols) mice. [^{3}H]ERGO remaining inside the intestinal lumen was measured by washing at 4 hr after oral administration. (B) Serial blood samples were collected at designated time intervals after the oral administration. Each value represents the mean ± SEM (n = 3 - 4).

Figure 2

Uptake of [^{3}H]ERGO from the apical side of small intestine.

(A) Uptake of [^{3}H]ERGO by each segment of small intestine of wild-type (closed columns) and *octn1*$^{-/-}$ (open columns) mice was measured for 10 min at 37°C. Data were normalized by [^{3}H]ERGO concentration in the medium and are shown as distribution volume. Each value represents the mean ± SEM (n = 4 - 6).

(B) Uptake of [^{3}H]ERGO in everted sacs of wild-type mice was measured in the absence (closed columns) or presence (shaded columns) of unlabeled ERGO at the designated

Downloaded from dmd.aspetjournals.org at ASPET Journals on April 19, 2024

DMD Fast Forward. Published on July 2, 2010 as DOI: 10.1124/dmd.110.032763
This article has not been copyedited and formatted. The final version may differ from this version.

concentrations. Data were normalized by the medium concentration, after subtraction of the uptake of [^{14}C]inulin. Each value represents the mean ± SEM (n = 3 - 8).

Figure 3

Inhibitory effect of TEA and verapamil on [^{3}H]ERGO uptake by everted sacs (A) and HEK293/OCTN1 cells (B).

(A) Everted sacs obtained from the upper and middle parts of small intestine of wild-type mice were incubated with [^{3}H]ERGO for 10 min at 37°C in the absence (closed column) or presence (shaded columns) of each compound, and uptake of [^{3}H]ERGO was measured. Data were normalized by the medium concentration, after subtraction of the uptake of [^{14}C]inulin. (B) HEK293/OCTN1 cells were incubated with [^{3}H]ERGO for 10 min at 37°C in the absence (closed column) or presence (shaded columns) of each compound, and uptake of [^{3}H]ERGO was measured. Data were normalized by medium concentration, after subtraction of the uptake of [^{3}H]ERGO observed in vector-transfected HEK293 cells to estimate OCTN1-mediated uptake. Each value represents the mean ± SEM (n = 3 - 8).

Figure 4

Downloaded from dmd.aspetjournals.org at ASPET Journals on April 19, 2024

DMD Fast Forward. Published on July 2, 2010 as DOI: 10.1124/dmd.110.032763
This article has not been copyedited and formatted. The final version may differ from this version.

Immunohistochemical analysis (A-J) and western blotting (K) of OCTN1 in mice

Cryosections of small intestine from wild-type (A, B, E, F, G, H, I, J) and *octn1*$^{-/-}$ (C, D) mice were incubated with antisera against OCTN1 (red), anti-Na^+/K^+ ATPase antibody (green in panel F, G) and antisera against PDZK1 (green in panel I, J). Panels B and D show merged images of the OCTN1 signal and bright-field image for wild-type (B) and *octn1*$^{-/-}$ (D) mice, respectively. Panel G is the merged image of OCTN1 (E) and Na^+/K^+ ATPase (F) for wild-type mice. Panel J is the merged image of OCTN1 (H) and PDZK1 (I) for wild-type mice. Note that the typical staining pattern of OCTN1 was observed in apical membrane of small intestine (A, E, G, H, I) in wild-type mice, but the staining was almost completely absent in *octn1*$^{-/-}$ mice (C). The lysates of intestinal BBMVs, hepatic NPC and PC were loaded onto SDS-PAGE (K). Bands corresponding to OCTN1 protein were detected in the samples of BBMVs and hepatic NPC, but not in that of PC.

Downloaded from dmd.aspetjournals.org at ASPET Journals on April 19, 2024

Figure 5

Immunohistochemical analysis of OCTN1 expression in human small intestine

Formalin-fixed and paraffin-embedded human small intestinal tissue slice was incubated with anti-OCTN1 antibody (A, C, D). The red signal shows OCTN1 immunostaining, and the blue

DMD Fast Forward. Published on July 2, 2010 as DOI: 10.1124/dmd.110.032763
This article has not been copyedited and formatted. The final version may differ from this version.

signal indicates cell nuclei (B, C). Panel D is a bright-field image.

Figure 6

Plasma concentration-time course (A) and cumulative urinary excretion (B) of [^{3}H]ERGO after intravenous administration.

[^{3}H]ERGO was intravenously administered to wild-type (closed circles) and *octn1*$^{-/-}$ (open circles) mice. Serial blood (A) and urine (B) samples were collected at designated time intervals after the intravenous administration. Each value represents the mean ± SEM (n = 4 - 6).

Figure 7

Integration plot representing initial distribution of [^{3}H]ERGO to the liver.

[^{3}H]ERGO was intravenously injected into wild-type (closed circles) and *octn1*$^{-/-}$ (open circles) mice. Liver and plasma concentrations were determined up to 5 min. CL_{uptake} was obtained from the slopes of the regression lines (showed as dotted lines). Each point represents separate experimental values obtained in a single mouse.

Downloaded from dmd.aspetjournals.org at ASPET Journals on April 19, 2024

DMD Fast Forward. Published on July 2, 2010 as DOI: 10.1124/dmd.110.032763
This article has not been copyedited and formatted. The final version may differ from this version.

Figure 8

Comparison of the uptake of [^{3}H]ERGO between isolated mouse liver PC (A) and NPC (B)

(A) PC freshly isolated from wild-type mice were incubated with [^{3}H]ERGO for the designated times, and the uptake was measured (closed circles). The uptakes of BSP (closed squares) and [^{14}C]inulin (closed triangles) were also examined as positive and negative controls. (B) NPC were freshly isolated from wild-type (closed symbols) and *octn1*$^{-/-}$ mice (open symbols) mice, and uptakes of [^{3}H]ERGO (circles) and [^{14}C]inulin (triangles) were measured. Each point was normalized by the medium concentration and represents the mean ± SEM (n = 3).

Figure 9

Immunohistochemical analysis of OCTN1 expression in mouse liver

Cryosections of liver obtained from wild-type mice were incubated with anti-OCTN1 (green) and anti-CD31 (red) antibodies. Blue signals indicate nuclei (G). Panels D, E, F and G are enlarged images. Note that OCTN1 exhibited a similar expression pattern in part to CD31 (C) and is partly colocalized with CD31 (F, G).

Downloaded from dmd.aspetjournals.org at ASPET Journals on April 19, 2024

DMD Fast Forward. Published on July 2, 2010 as DOI: 10.1124/dmd.110.032763
This article has not been copyedited and formatted. The final version may differ from this version.

Table 1. Tissue-to-plasma concentration ratio (Kp) of [^{3}H]ERGO after intravenous administration[a)]

	Kp (mL/g tissue)[a)]	
	wild-type	*octn1*$^{-/-}$
Liver	238 ± 25	6.69 ± 1.73 *
Kidney	79.4 ± 6.6	12.4 ± 1.3 *
Spleen	23.4 ± 3.2	1.62 ± 0.46 *
Lung	10.7 ± 2.1	1.70 ± 0.42 *
Heart	3.10 ± 0.23	0.993 ± 0.432 *
Intestine (Upper)	12.4 ± 1.6	1.99 ± 0.37 *
Intestine (Middle)	19.5 ± 0.7	3.37 ± 0.93 *
Intestine (Lower)	19.2 ± 1.9	2.04 ± 1.04 *
Large Intestine	7.45 ± 0.67	1.78 ± 0.87 *
Testis	1.75 ± 0.08	0.715 ± 0.151 *
Pancreas	9.48 ± 1.19	1.45 ± 0.41 *
Thymus	5.98 ± 1.38	1.07 ± 0.27 *
Muscle	2.04 ± 0.27	1.11 ± 0.40
Brain	0.425 ± 0.029	0.539 ± 0.216
Bone Marrow	30.7 ± 6.0	1.78 ± 1.30 *
Blood	1.30 ± 0.13	0.763 ± 0.044 *

a) Kp values were obtained 4 hr after administration (mean ± SEM, n = 3 - 4).

*, Significantly different from wild-type mice ($p < 0.05$).

Downloaded from dmd.aspetjournals.org at ASPET Journals on April 19, 2024

Figure 1

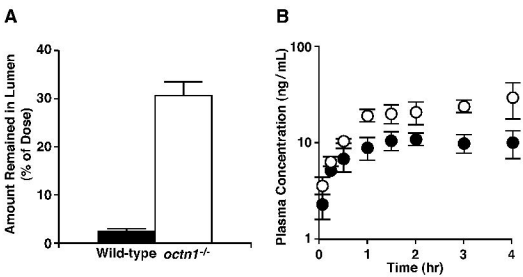
A
Amount Remained in Lumen (% of Dose)
40
30
20
10
0
Wild-type
octn1-/-
B
Plasma Concentration (ng/mL)
100
10
1
0
1
2
3
4
Time (hr)

Figure 2

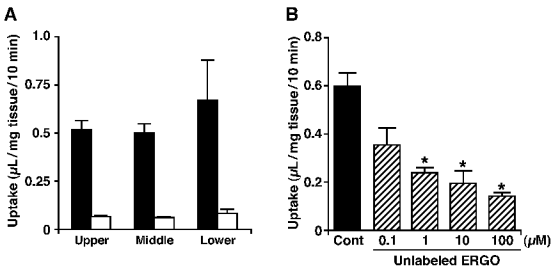
A
Uptake (μL/mg tissue/10 min)
1.0
0.75
0.5
0.25
0
Upper
Middle
Lower
B
Uptake (μL/mg tissue/10 min)
0.8
0.6
0.4
0.2
0
Cont
0.1
1
10
100
(μM)
Unlabeled ERGO
*
*
*

Figure 3

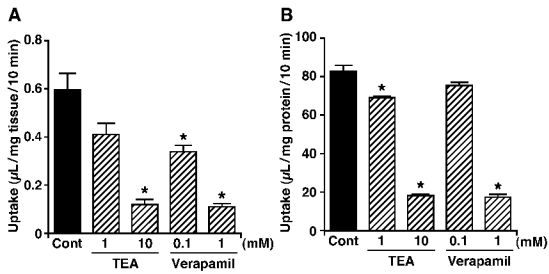
A
Uptake (μL/mg tissue/10 min)
0.8
0.6
0.4
0.2
0
Cont
1
10
0.1
1
(mM)
TEA
Verapamil
*
B
Uptake (μL/mg protein/10 min)
100
80
60
40
20
0
Cont
1
10
0.1
1
(mM)
TEA
Verapamil
*

Figure 4

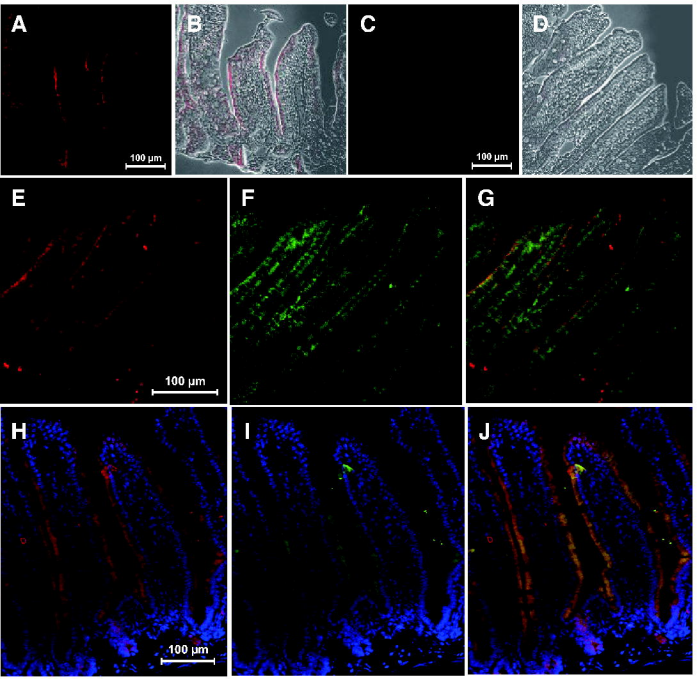
A
B
C
D
100 μm
100 μm
E
F
G
100 μm
H
I
J
100 μm

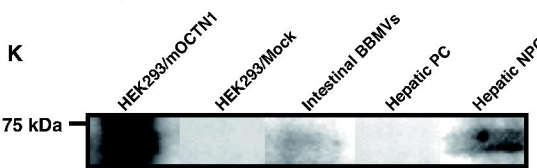
K
HEK293/mOCTN1
HEK293/Mock
Intestinal BBMVs
Hepatic PC
Hepatic NPC
75 kDa

Figure 5

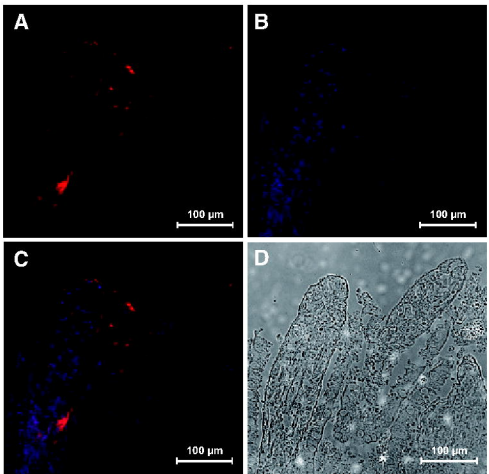

Figure 6

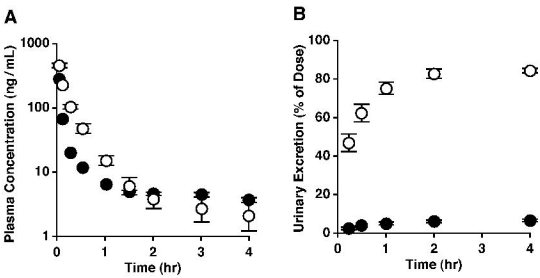
A
Plasma Concentration (ng/mL)
1000
100
10
1
0
1
2
3
4
Time (hr)
B
Urinary Excretion (% of Dose)
100
80
60
40
20
0
0
1
2
3
4
Time (hr)

Figure 7

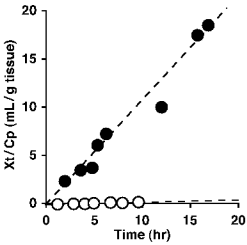

Figure 8

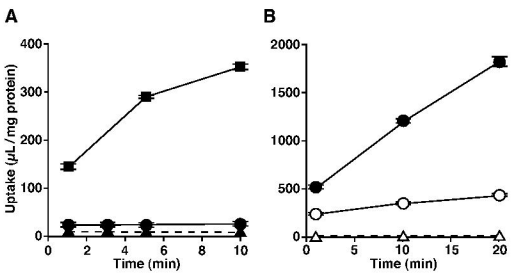
A
B
Uptake (µL / mg protein)
Time (min)
Time (min)
0
100
200
300
400
500
1000
1500
2000
0
2
4
6
8
10
0
5
10
15
20

Figure 9